Electronic Supplementary Information (ESI)

In this Electronic Supplementary Information (ESI) we provide additional simulation results. The corresponding figures are referred to as "Supplementary Materials" in the main text of the article. Here the figures are ordered according to their sequence in the text.

III A: Dynamin as cuff-shaped potential

III B: Dynamin as rings of amphiphilic discs – 2. Two rings

We also investigated the orientation of the amphiphilic disks on the membrane by monitoring the angle, θ, between the orientation vector and the vector defining the shortest connection from the cylinder axis to the peptide's center of mass. While this angle does not include information on the exact orientation in space, it can be assumed that the preferential direction will be determined by the inclination of the membrane at the peptides' location (cf. Fig. 14), which will give the peptides a tilt towards the direction in which the largest amount of constriction is induced. Table 4 gives a summary of the results for the different systems we simulated. While θ is generally relatively small, its values coincide nicely with the amount of

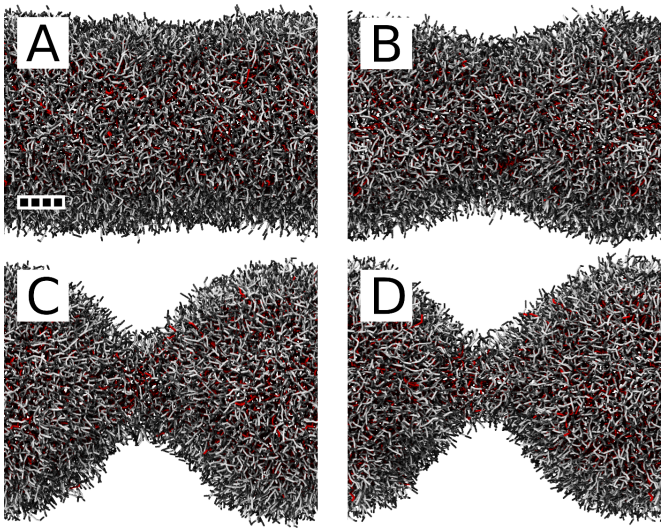

Fig. 20 Deformation caused in a cylindrical lipid bilayer by a $2\,\sigma$ long cuff potential constricting with a constant velocity of $0.001\,\sigma\tau^{-1}$. Head-group beads are shown in black, and tails belonging to the inner and outer monolayer in red and gray, respectively. The snapshots show the process from the unperturbed system (A) over increasing stages of constriction (B, C) up until the point at which the inner head-group beads meet (D). The subsequent topological changes of the process are shown at higher detail in Fig. 6. The patterned bar shown in the lower left of A corresponds to a distance of $4\,\sigma$.

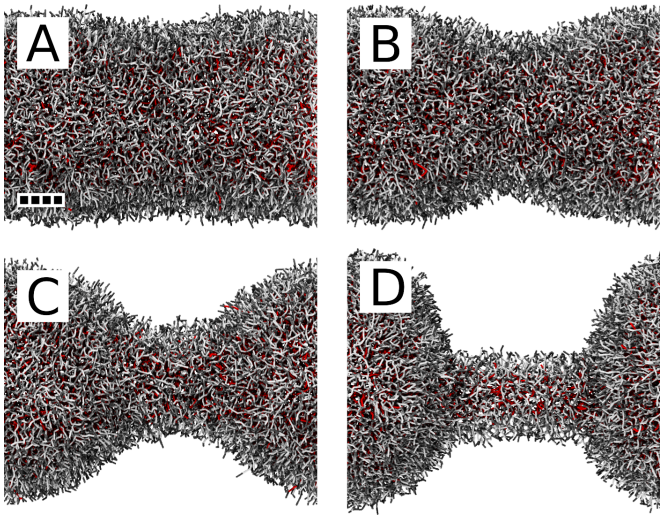

Fig. 21 Deformation caused in a cylindrical lipid bilayer by a $2\,\sigma$ long cuff potential constricting with a constant velocity of $0.001\,\sigma\tau^{-1}$ while simultaneously elongating at a rate that the cuff area remains constant. Headgroup beads are shown in black, and tails belonging to the inner and outer monolayer in red and gray, respectively. The snapshots show the process from the unperturbed system (A) over increasing stages of constriction (B, C) up until the point at which the inner head-group beads meet (D). The subsequent topological changes of the process are shown at higher detail in Fig. 8. The patterned bar shown in the lower left of A corresponds to a distance of $4\,\sigma$.

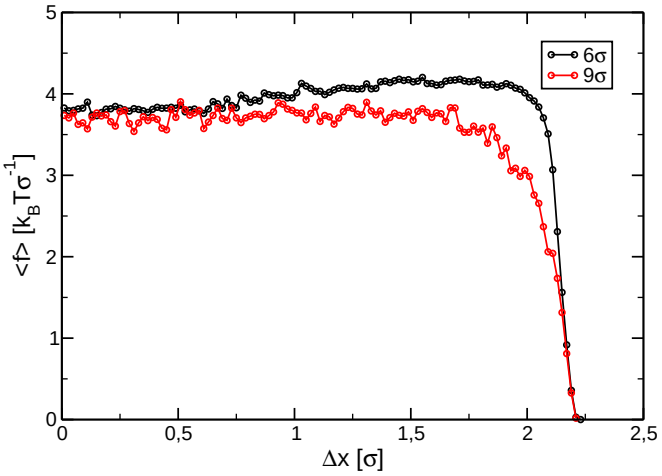

Fig. 22 Plot of the average force $\langle f \rangle$ the cuff potential exerts on the lipid beads in dependence on its position along the cylinder axis, defined by its displacement Δx from the cuff's center. The length l_c of the cylindrical mantle around which the cuff potential is defined was $2\,\sigma$, and the cuff's radius was set to the values given in the legend. Note that the cuff's mantle ends at $\Delta x = 1\,\sigma$.

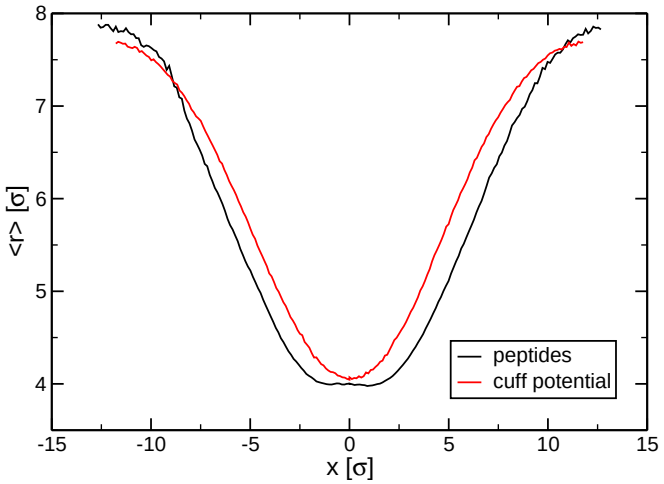

Fig. 23 Average radii r of membrane tubes (center to bilayer's midplane) around the x axis. Shown is a system constricted by a cuff potential using a cylinder length of $2\,\sigma$ and a radius of $8\,\sigma$, compared to a system constricted using a ring of amphiphilic disks with a ring radius of $5.5\,\sigma$. As befits the similar profile shapes, the perpendicular force exerted by the cuff potential is $38.32\,k_{\mathrm{B}}T\,\sigma^{-2}$, which is very close to the force of $36,48\,k_{\mathrm{B}}T\,\sigma^{-2}$ exerted by the peptide disks.

constriction generated on top of the constriction caused by the ring radius, and the system combining a ring radius of $5\,\sigma$ and a separation of $6\,\sigma$, which displays the most significant additional constriction, also has the largest tilt for the peptides.

Table 4 Average angle θ and its standard deviation between the orientation vector and the vector defining the shortest connection from the cylinder axis to the peptide's center of mass for our simulations with two peptide rings with radius R and a separation of d.

R [σ]	d [σ]	$\langle\theta\rangle$	SD(θ)
5	6	0.29	0.14
5	10	0.24	0.13
5	12	0.23	0.12
8	6	0.20	0.11
8	10	0.22	0.12
8	12	0.23	0.12